JOURNAL OF GEOPHYSICAL RESEARCH, VOL. 112, C10006, doi:10.1029/2006JC003803, 2007

Oceanic distribution and sources of bromoform and dibromomethane in the Mauritanian upwelling

Birgit Quack,[1] Ilka Peeken,[1] Gert Petrick,[1] and Kerstin Nachtigall[1]

Received 6 July 2006; revised 22 February 2007; accepted 31 May 2007; published 6 October 2007.

[1] The tropical oceans are a source of reactive bromine to the atmosphere in the form of short-lived brominated methanes as bromoform ($CHBr_3$) and dibromomethane (CH_2Br_2). Elevated atmospheric concentrations above the tropical oceans are related to oceanic supersaturations of the compounds and especially to upwelling regimes. Although the sources of these brominated gases in the open ocean are not well understood, they have been habitually linked to phytoplankton, especially diatom abundance. Thus according to common assumptions, high concentrations of the brominated trace gases were expected to occur in the biologically active and diatom-rich Mauritanian upwelling. However, contrary to expectations, only low levels were encountered in the upwelling waters, 10.7 (range 5.2–23.8) pmol L^{-1} $CHBr_3$ and 4.7 (range 3.1–7.0) pmol L^{-1} CH_2Br_2, values more typical of open ocean concentrations. The aqueous $CHBr_3$ concentrations were not correlated to high chlorophyll *a* values or diatom abundances. However, significant correlations existed with low concentrations of marker pigments for diatoms, cyanobacteria, and degradation, suggesting miscellaneous small biological sources of the compound in the upwelling. Air-sea exchange could additionally account for an oceanic source in fresh upwelled waters, while advection of different water masses also influenced the distribution. $CHBr_3$ concentrations were maximized in warm and nitrogen-depleted surface waters, while CH_2Br_2 was maximized in colder and nitrogen-enriched deeper waters, suggesting that both compounds, at least in part, have different sources and fates.

Citation: Quack, B., I. Peeken, G. Petrick, and K. Nachtigall (2007), Oceanic distribution and sources of bromoform and dibromomethane in the Mauritanian upwelling, *J. Geophys. Res.*, *112*, C10006, doi:10.1029/2006JC003803.

1. Introduction

[2] The short-lived brominated methanes bromoform ($CHBr_3$) and dibromomethane (CH_2Br_2) are recognized as representing an important source of bromine to the troposphere and lower stratosphere [*World Meteorological Organization*, 2007; *Salawitch*, 2006]. These compounds represent the largest natural contributions to atmospheric organic bromine and may contribute 20–30% to stratospheric and tropospheric O_3 depletion [*Salawitch et al.*, 2005; *Yang et al.*, 2005]. The magnitude of the oceanic emissions is uncertain and the spatial and temporal distributions of these compounds are not well understood [*Quack and Wallace*, 2003]. Maxima of atmospheric $CHBr_3$ have been observed over the tropical oceans [*Atlas et al.*, 1993; *Schauffler et al.*, 1999; *Class and Ballschmiter*, 1988] and these maxima were linked to productive upwelling areas. Equatorial surface waters of the tropical Atlantic were indeed identified as a significant $CHBr_3$ source to the atmosphere, with $CHBr_3$ production occurring in the deep chlorophyll maximum [*Quack et al.*, 2004]. Elevated concentrations of $CHBr_3$ and CH_2Br_2 in the open ocean are often linked to phytoplankton; particularly diatoms [*Baker et al.*, 2000; *Atlas et al.*, 1993; *Klick and Abrahamsson*, 1992; *Class and Ballschmiter*, 1988] for which laboratory studies with cultures have also shown production of $CHBr_3$ [*Moore et al.*, 1996]. Advection of coastal waters enriched in macro algal $CHBr_3$ [*Carpenter and Liss*, 2000], emissions of floating macro algae [*Moore and Tokarczyk*, 1993] and decay of organic matter [*Quack and Wallace*, 2003] are suggested as other possible causes for open ocean supersaturations of the compound. In coastal regions macro algae are thought to be its major marine sources [*Manley et al.*, 1992; *Nightingale et al.*, 1995; *Carpenter and Liss*, 2000], while anthropogenic contamination by industrial or municipal effluents may overwhelm the natural sources in some areas [*Quack and Wallace*, 2003].

[3] Biological production of both compounds occurs during the enzymatic oxidation of bromine by bromoperoxidases and chloroperoxidases in the presence of hydrogen peroxide, resulting in the halogenation of organic compounds with activated terminal methyl groups [*Neidleman and Geigert*, 1986; *Theiler et al.*, 1978]. This principle resembles the haloform reaction, where chemical oxidation of bromide is followed by bromination of organic substrates and hydrolyzation of the unstable intermediates to CH_2Br_2 and mainly $CHBr_3$ in alkaline solutions. The formation of

[1]Department of Marine Biogeochemistry, Leibniz-Institute of Marine Sciences, Kiel, Germany.

0148-0227/07/2006JC003803$09.00

$CHBr_3$ during the oxidation of organic matter is chemically favored over CH_2Br_2, since intermediate products are stabilized by additional halogen atoms, and thus $CHBr_3$ is expected to be the major product in oceanic environments [*Wade*, 1999].

[4] Biogenic CH_2Br_2 has been identified as a minor product from phytoplankton and macro algae cultures [*Tokarczyk and Moore*, 1994; *Manley et al.*, 1992], and is generally considered as a side product during $CHBr_3$ production [*Theiler et al.*, 1978]. A further process generating CH_2Br_2 is reductive hydrogenolysis of $CHBr_3$, which occurs mainly in anoxic environments [*Vogel et al.*, 1987; *Tanhua et al.*, 1996].

[5] Losses of the brominated methane compounds from the oceanic mixed layer include physical air-sea exchange and turbulent mixing (half-lives of days to weeks [*Quack and Wallace*, 2003; *Quack et al.*, 2004]), with slower chemical conversion losses from hydrolysis (half-lives of 183 years for CH_2Br_2 and 686 years for $CHBr_3$ [*Mabey and Mill*, 1978]) and halogen exchange (half-live of 5–74 years for $CHBr_3$ [*Geen*, 1992]) as well as biodegradation under aerobic and anaerobic conditions [*Bouwer and McCarty*, 1983; *Bartnicki and Castro*, 1994; *Goodwin et al.*, 1997]. $CHBr_3$ has generally longer lifetimes compared to CH_2Br_2 in the oceanic environment and only the rate of reduction is faster for $CHBr_3$ than for CH_2Br_2 [*Vogel et al.*, 1987].

[6] In order to investigate the Mauritanian upwelling as a source of radiatively and chemically active atmospheric trace gases, a cruise was conducted with R/V *Poseidon* in March/April 2005. Together with the brominated halocarbons in water and air, the distribution of phytoplankton pigments and ancillary chemical parameters were measured. Here we present the oceanic measurements of CH_2Br_2 and $CHBr_3$ in the water column of the upwelling area and discuss their distributions and the few significant correlations with geographical, physical, chemical (nutrients and oxygen) and biological (phytoplankton pigments) variables.

2. Study Area

2.1. Hydrography

[7] A 50 km wide shelf (coast to 200–300 m depth), carved by under water canyons, characterizes the Mauritanian upwelling from 16°–19.5°N. The Banc D'Arguin region (19.5°–21.5°N) is characterized by a gently sloping shelf (coast to 50 m depth) of 130 km width. This region shows intense seasonal upwelling during late winter and spring, induced by the North East trade winds [*Demarcq and Faure*, 2000]. Strength of the upwelling fluctuates on multiday, interannual and decadal atmospheric variations [*Hagen*, 2001] and is influenced by wind variations, tidal processes and small-scale bottom topographic features such as submarine canyons [*Postel and Zahn*, 1987].

[8] This upwelling system is probably the most complex of all coastal upwelling systems, particularly near Cape Blanc (20°N) where the frontal zone between the salty (>35) North Atlantic Central Water (NACW) and less salty (<35), nutrient-rich South Atlantic Central Water (SACW) reaches the African coast. The upwelling of the Mauritanian coast is mainly fed by SACW from 50 to 300 m depth in spring [*Minas et al.*, 1982], which mixes gradually with nutrient-depleted warm surface water of the open tropical ocean. The result is an extremely patchy distribution of physical, chemical and biological parameters in the upwelling surface waters.

2.2. Plankton

[9] As freshly upwelled nutrient-rich water ages and mixes with nutrient-depleted warm water from the tropical open ocean a succession of phytoplankton species develops in the surface waters around the core of maximum upwelling. Small diatoms appear first, sometimes accompanied by the prymnesiophyte *Phaeocystis* sp. Under subsequent stratifying conditions larger diatoms appear, with an increasing proportion of prymnesiophytes including coccolithophorids, and finally dinoflagellates, which are adapted to low-nutrient conditions at the periphery of the upwelling zone [*Margaleff*, 1978; *Gibb et al.*, 2000]. The entrainment of nutrient-depleted warm surface water from the open ocean introduces large amounts of cyanobacteria (*Synechococcus* sp., *Trichodesmium* sp.). *Synechococcus* sp. are enhanced in the upwelling in spring [*Gibb et al.*, 2000], while prochlorophytes are always weak (4–16%) [*Partensky et al.*, 1996]. Generally, the distribution of phytoplankton is very patchy and communities change over short distances.

[10] Marker pigments can be used to characterize plankton populations and processes [*Jeffrey et al.*, 1997]. In the upwelling 19-hexanoylfucoxanthin (prymnesiophytes), 19-butanoylfucoxanthin (chrysophytes), zeaxanthin (cyanobacteria and prochlorophytes), chlorophyll *b* (green flagellates) and peridin (dinoflagellates) accompany chlorophyll *a* and fucoxanthin (diatoms) [*Barlow et al.*, 2004]. Phaeopigments are indicative of grazing and phytoplankton senescence, related to digestion by animals and microbial transformations [*Roy and Poulet*, 1990].

3. Method

[11] Bromoform ($CHBr_3$) and dibromomethane (CH_2Br_2) were measured in the water column of the Mauritanian upwelling during cruise P320/1 of R/V *Poseidon* from Las Palmas/Canary Islands, 21 March 2005 to Mindelo/Cape Verde Islands, 7 April 2005. Thirty-two CTD stations were sampled along the cruise track (Figure 1) for hydrographic parameters. Water samples were collected from 10 L Niskin bottles, mounted on a 12-bottle CTD rosette package. Nutrients were analyzed photometrically with an auto analyzer. Oxygen was analyzed by Winkler titration [*Grasshoff et al.*, 1999].

[12] Halocarbon data were obtained at 20 stations between 1 and 3000 m depth. The samples were analyzed on board, using a purge and trap multidimensional GC/MS analytical system, equipped with a parallel Electron Capture Detector (ECD). The bromocarbons were quantified in single ion mode. Quantification was performed with volumetrically prepared standards in methanol. More details of the analytical system are described by *Quack et al.* [2004, 2007].

[13] For phytoplankton pigment analysis, 1–2 L of water were filtered through GF/F filters, which were stored at −80°C until they were analyzed via high-performance liquid chromatography (HPLC), details are described by *Hoffmann et al.* [2006].

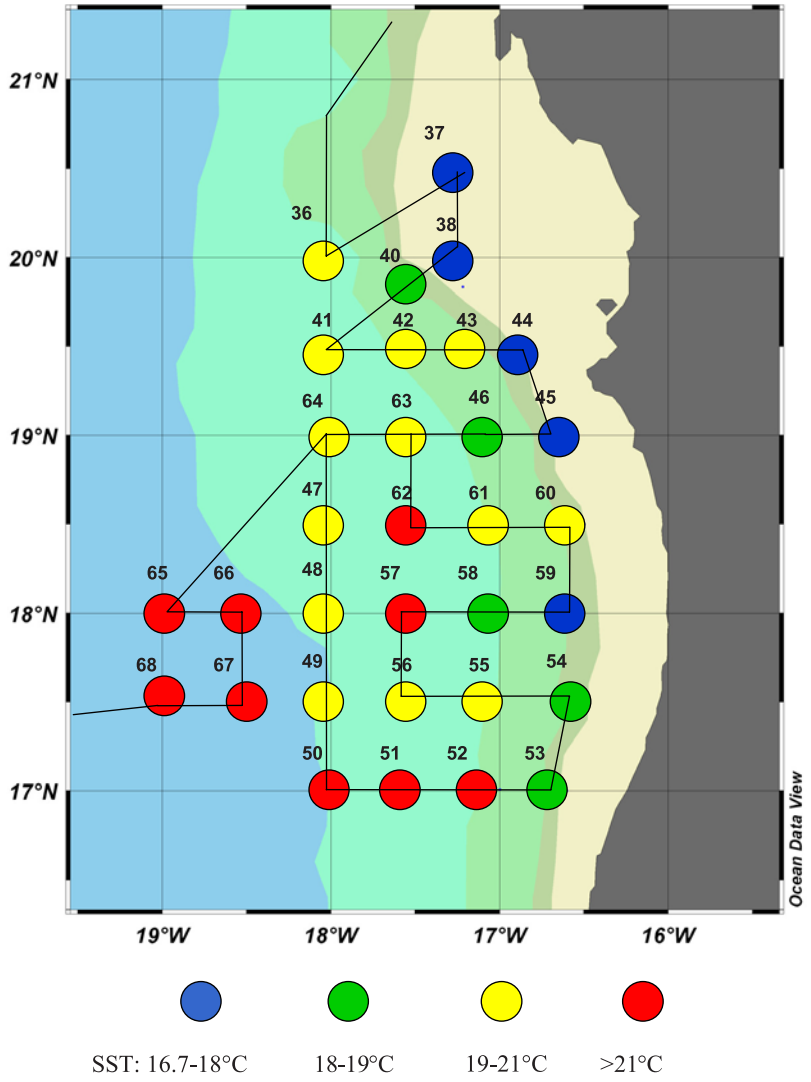

Figure 1. Track and stations of *Poseidon* cruise 320/1 in the Mauritanian upwelling (March/April 2005). Color identifies sea surface temperature (SST) clusters: dark blue (fresh upwelled water, SST 16.7°–18°C), green (aged upwelled water, SST 18°C–19°C), yellow (mixed water, SST 19°–21°C), and red (nutrient-depleted warm water, SST >21°C). Shading indicates ocean bathymetry, blue (>3000 m), dark green (2000–3000 m), green (1000–2000 m), light green (500–1000 m), yellow (<500 m), and grey (land).

[14] The taxonomic structure of phytoplankton communities was derived from photosynthetic pigment ratios using the CHEMTAX® program [*Mackey et al.*, 1996] applying the input matrix of *Veldhuis and Kraay* [2004]. The phytoplankton group composition is expressed in chlorophyll *a* concentrations.

4. Results

4.1. Station Cluster

[15] Water masses with different chemical and biological properties of all trophic stages are found in close proximity in the Mauritanian upwelling. In order to improve the visualization of the data set and to increase the conformity of chemical or biological variables for correlation analysis the entire data set was divided into four station clusters (Figure 1 and Table 1). Sea surface temperature (SST) served as division criterion, since it reflects the history of cold upwelled water (16.7°C), as it ages and mixes with the open ocean surface water (22°C). Station clusters thus represent different water types of fresh upwelled waters at the coast (cluster 1: 16.7°–18°C), aged upwelled (cluster 2: 18°–19°C), mixed water types (cluster 3: 19°–21°C) and nutrient-depleted open ocean water entrainments (cluster 4: >21°C).

4.2. Chemical and Biological Background During *Poseidon* Cruise 320/1

[16] Chemical signatures and biological characteristics differed considerably between fresh upwelled water (16.7°C), the aging upwelled waters and nutrient-depleted warm surface waters (22°C) in the Mauritanian upwelling area (Table 1). While the highest nitrate (NO_3^-) concentrations of up to 18 μmol L^{-1} were found in fresh upwelled surface water (0–12 m), NO_3^- mean values decreased from 6.5 μmol L^{-1} in the aged upwelled waters to 0.3 μmol L^{-1}

Table 1. Values of Physical, Chemical, and Biological Variables in Different Depth Ranges (0–12 m and 14–50 m) of Four SST Clusters in the Mauritanian Upwelling[a]

Parameter	Entire data	Minimum	Maximum	Cluster 1	Cluster 2	Cluster 3	Cluster 4
			Depth Range 0–12 m				
Temperature, °C	19.4	16.8	21.8	17.4	18.6	20.1	21.2
Salinity	35.74	19.98	36.13	35.10	35.86	36.02	35.99
CH_2Br_2, pmol L^{-1}	4.9	3.1	7.0	5.0	4.5	4.6	5.2
$CHBr_3$, pmol L^{-1}	10.7	5.2	23.8	9.6	9.3	11.0	13.1
$CH_2Br_2/CHBr_3$	0.51	0.15	1.06	0.56	0.57	0.52	0.40
Oxygen, μmol L^{-1}	218	138	263	165	247	237	235
AOU, μmol L^{-1}	14	−27	102	76	−12	−8	−11
Nitrate, μmol L^{-1}	4.4	0.0	18.3	15.8	6.5	1.7	0.3
Phosphate, μmol L^{-1}	0.4	0.1	1.3	1.2	0.5	0.3	0.2
Sum chlorophyll *a*, μg L^{-1}	2.56	0.07	11.22	2.45	7.26	1.81	0.84
Fucoxanthin, ng L^{-1}	1159	24	6826	837	4064	789	165
Peridin, ng L^{-1}	77	0	422	29	154	92	51
19-butanoylfucoxanthin, ng L^{-1}	39	0	513	0	16	74	37
19-hexanoylfucoxanthin, ng L^{-1}	194	0	786	102	200	269	165
Zeaxanthin, ng L^{-1}	98	4	487	55	36	118	141
Chlorophyll *b*, ng L^{-1}	149	0	1344	239	122	150	91
Sum phaeopigments, ng L^{-1}	374	9	2848	363	1390	172	44
			Depth Range 14–50 m				
Temperature, °C	18.1	14.7	21.4	16.6	17.2	18.2	19.4
Salinity	35.92	35.49	36.32	35.87	35.78	35.95	35.98
CH_2Br_2, pmol L^{-1}	5.8	2.1	11.8	5.0	6.2	6.6	5.0
$CHBr_3$, pmol L^{-1}	9.0	4.6	12.8	10.8	7.6	8.3	9.8
$CH_2Br_2/CHBr_3$	0.67	0.21	1.18	0.47	0.81	0.80	0.51
Oxygen, μmol L^{-1}	160	60	247	123	147	170	179
AOU, μmol L^{-1}	76	−15	188	118	93	65	52
Nitrate, μmol L^{-1}	11.8	0.0	24.8	19.2	14.9	11.0	8.5
Phosphate, μmol L^{-1}	0.9	0.1	1.9	1.3	1.0	0.8	0.7
Sum chlorophyll *a*, μg L^{-1}	1.26	0.05	8.22	0.84	3.00	1.05	0.82
Fucoxanthin, ng L^{-1}	534	21	3729	369	1395	470	240
Peridin, ng L^{-1}	60	0	1168	12	22	99	53
19-Butanoylfucoxanthin, ng L^{-1}	19	0	106	0	1	20	38
19-Hexanoylfucoxanthin, ng L^{-1}	101	0	727	27	52	124	134
Zeaxanthin, ng L^{-1}	47	0	437	8	13	53	77
Chlorophyll *b*, ng L^{-1}	73	0	274	63	39	69	101
Sum phaeopigments, ng L^{-1}	239	7	1674	277	650	188	69

[a]Cluster 1 (fresh upwelled water, SST 16.7°–18°C), cluster 2 (aged upwelled water, SST 18°C–19°C), cluster 3 (mixed water, SST 19°–21°C), cluster 4 (nutrient-depleted warm water, SST >21°C).

in the open ocean waters of the same depth range. Despite the high nutrient load, the highest phytoplankton biomass was observed in the aged upwelled waters with a maximum of 11 μg chlorophyll *a* L^{-1} and an average of about 7 μg L^{-1} (Figure 2). The second highest biomass was found in fresh upwelled waters (chl *a*: 2.5 μg L^{-1}), while the lowest chlorophyll biomass was encountered in open ocean waters (chl *a*: 0.8 μg L^{-1}). This value is still high compared to normal oligotrophic background measurements in the tropical Atlantic [*Fernández et al.*, 2003; *Gibb et al.*, 2001; *Marañón et al.*, 2000]. Below 14 m, chlorophyll concentrations were always lower compared to the surface with mean values of about 1.0 μg L^{-1}, while the highest concentration of 3 μg L^{-1} was again found in the aged upwelled waters of cluster 2 (Figure 2).

[17] A distinct phytoplankton distribution was detected for each cluster. The highest contribution from diatoms was found in the aged upwelled water both in surface and deep communities. The fresh upwelled waters also contained a high diatom load in the surface and the deep water, while their contribution decreased in the mixed waters and was absent in the surface open ocean waters (Figure 2). The diatom population consisted of small diatoms (e.g., *Thalassiosira* sp.) in fresh upwelled waters (cluster 1), with a large fraction of broken diatom frustules in the north of the investigation area. In the aged upwelled waters (cluster 2) in the southeast, the region with the highest diatom contribution, a few diatom species dominated (e.g., *Leptocylindrus* sp., *Nitzschia* sp.), while different species occurred in the northwest (e.g., *Guardina deliculata, Thallssiosira* sp., *Odontella mobiliensis*). Mesotrophic conditions at the edge of the upwelling zone (cluster 3) favored larger diatoms (e.g., *Proboscia alata*).

[18] In mixed and Open Ocean waters (clusters 3 and 4) prymnesiophytes and cyanobacteria dominated the phytoplankton community and reached up to 50% of the total biomass in cluster 4. Prochlorophytes were of minor importance in the entire investigation area, never exceeding 2% of the phytoplankton community. While cryptophytes and prasinophytes were always present, chlorophytes were generally restricted to the aged upwelled waters. Autotrophic dinoflagellates and pelagophytes mainly occurred in the mixed and open waters and had a higher contribution in the deep waters compared to the surface.

[19] Good correlations ($r^2 > 0.8$) between the diatom marker fucoxanthin and phaeopigments (phaeophorpide, pyro-phaeophorbide, phaeophytin, pyro-phaeophytin) suggests active populations of diatom grazers in the upwelling waters (e.g., Figure 3). Zooplankton was not explicitly investigated during our cruise, however small copepods,

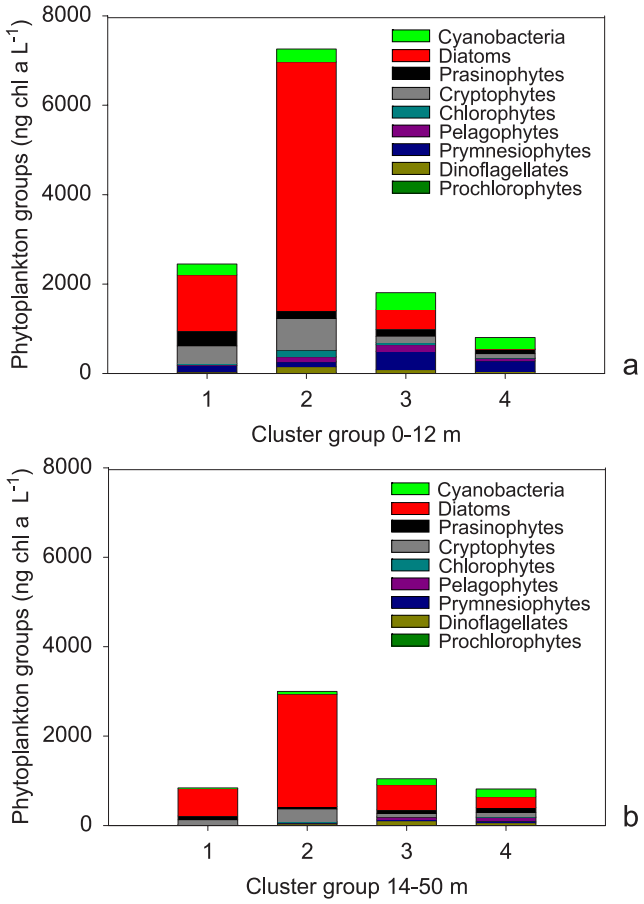

Figure 2. Phytoplankton composition (based on marker pigments) expressed in chlorophyll *a* for (a) the surface 0–12 m and (b) the deeper water column 14–50 m of four SST-based clusters (for details see text and Figure 1). Color code is as follows: cyanobacteria (light green), diatoms (red), prasinophytes (black), cryptophytes (grey), chlorophytes (ocean blue), pelagophytes (pink), prymnesiophytes (dark blue), dinoflagelates (green brown), and prochlorophytes (dark green).

which are known to live in large patchy populations in the upwelling region [*Weikert*, 1984], could often be seen on the pigment filter samples.

4.3. Oceanic Distributions of $CHBr_3$ and CH_2Br_2 in the Mauritanian Upwelling

[20] Both $CHBr_3$ and CH_2Br_2 showed vertical and horizontal gradients in the different waters of the Mauritanian upwelling. Concentrations of $CHBr_3$ (5.2 to 23.8 pmol L^{-1}) were low and generally increased toward the surface and toward warmer waters of higher salinity while elevated concentrations accumulated in waters >17°C with a salinity >35.8 (Figures 4a and 5a and Table 1). Lowest concentrations were found in the most intense upwelling surface waters (mean 9.6 pmol L^{-1}) and in slightly aged upwelled waters (mean 9.3 pmol L^{-1}) with high phytoplankton (diatom) abundance and concentrations increased offshore toward nutrient-depleted warm surface waters (mean: 13.1 pmol L^{-1}). In the fresh upwelled waters close to the coast $CHBr_3$ concentrations increased toward the north.

[21] Concentrations of CH_2Br_2 (3.1 to 7.0 pmol L^{-1}) generally increased toward the coast and were greater at depth (14–50 m) than in near surface waters (0–12 m) with high concentrations accumulating in colder water SST <17°C with low salinity (<36.5) (Figures 4b and 5b and Table 1). The CH_2Br_2 to $CHBr_3$ ratio (0.15–1.06) increased with depth and with colder more saline waters (Figures 4c and 5c); the highest ratio (>0.8) was found in waters of 15°–17°C with salinity of 35.8–35.9. The CH_2Br_2 and $CHBr_3$ distributions show opposite patterns in different water types toward different depths (Figure 6).

[22] Depth profiles of $CHBr_3$ and CH_2Br_2 revealed different distributions (here denoted Type A and B) of the compounds among the stations (Figure 7). Type A profiles showed maximum $CHBr_3$ concentrations at the depth of the mixed layer (density gradient of $\Delta\sigma_\theta > 0.1$, e.g., stations 60 and 66) (Figure 7a), while CH_2Br_2 concentrations increased below this mixed layer. The mixed layer in the Mauritanian upwelling ranged from 15 m at the coast to 37 m offshore, and was often defined (>66% of the stations) by a weaker density gradient of $\Delta\sigma_\theta < 0.05$. At these stations (type B profiles, Figure 7b) profiles of the brominated compounds were relatively uniform with maxima of $CHBr_3$ below the mixed layer in the upper thermocline at 30 to 50 m depth (e.g., stations 54, 55, 59).

5. Discussion on Possible Sources of $CHBr_3$ and CH_2Br_2

[23] The distributions of $CHBr_3$ and CH_2Br_2 in the upwelling region are affected by many processes, including

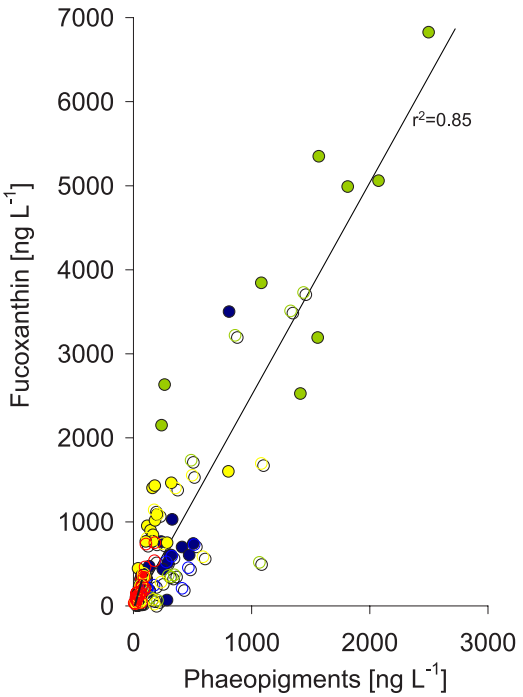

Figure 3. Fucoxanthin versus the sum of phaeopigments in the Mauritanian upwelling during March/April 2005. Correlation of the entire data set is $r^2 = 0.85$. (Colors mark different SST clusters: 0–12 m (solid circles) and 14–50 m (open circles); see Figure 1).

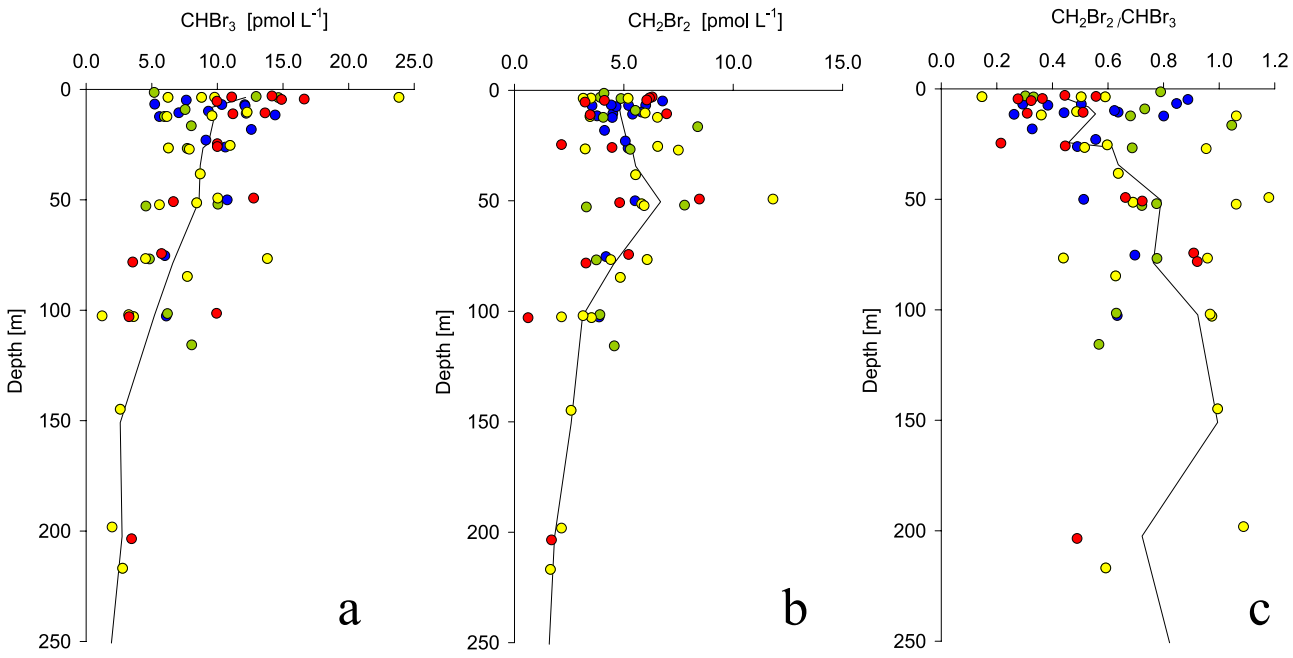

Figure 4. Distribution of $CHBr_3$ and CH_2Br_2 in the Mauritanian upwelling: $CHBr_3$ versus (a) depth, (b) CH_2Br_2 versus depth, and (c) the ratio $CH_2Br_2/CHBr_3$ versus depth. Mean values of the entire data set per 10 m are indicated as black lines. (Colors mark different SST clusters; see Figure 1).

advection, plankton distribution, degradation of organic matter, air-sea exchange and mixing [*Quack and Wallace*, 2003; *Quack et al.*, 2004]. Although the concentrations in the present study are small, showing that the overall production of the compounds in the Mauritanian upwelling is low, observations and interpretations of correlations suggest that sources for $CHBr_3$ and CH_2Br_2 exist in this region.

[24] Correlation analyses were performed for $CHBr_3$ and CH_2Br_2 for a surface depth range (0–12 m) and a surface column range (0–100 m) of the entire data set and the different station clusters. Significant correlations ($p < 0.05$) are summarized in Table 2. The heterogeneity of the Mauritanian upwelling and the complexity of the processes produce complex correlations among various biological and chemical parameters (Table 2). In the following we discuss individual processes and correlations, their influence on the $CHBr_3$ and CH_2Br_2 distributions and possible source processes for the compounds. Among these processes are the air-sea exchange of the two bromoinated compounds, which is covered in a separate paper [*Quack et al.*, 2007], the correlation with physical and biogeochemical tracers and the correlation with biological variables.

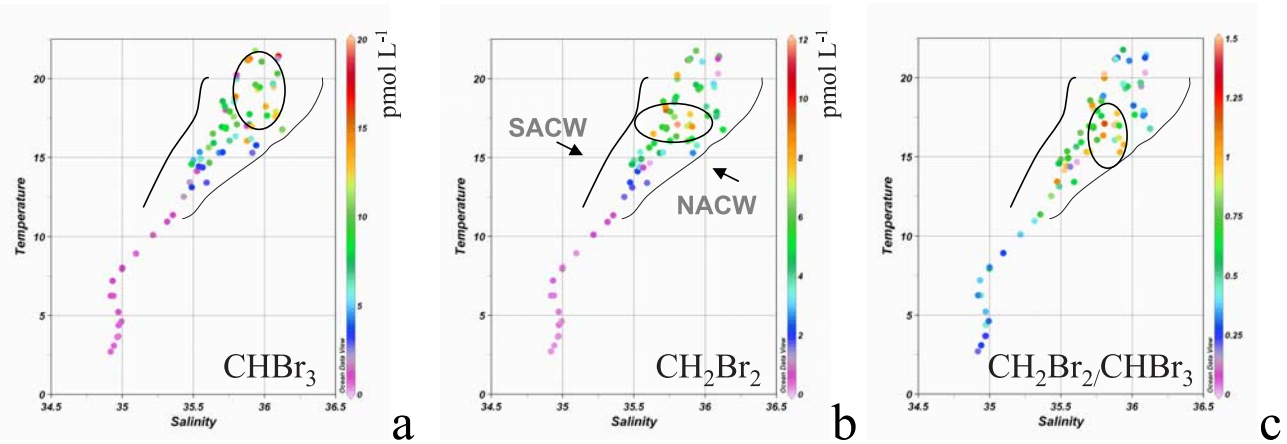

Figure 5. Concentrations of halocarbons in different water masses of the Mauritanian upwelling: (a) $CHBr_3$ in the temperature (T)/salinity (S) diagram, (b) CH_2Br_2 in the T/S diagram, and (c) $CH_2Br_2/CHBr_3$ in the T/S diagram. Black lines mark T/S properties of North Atlantic Central Water (NACW) and South Atlantic Central Water (SACW). Circles mark the accumulation of high values.

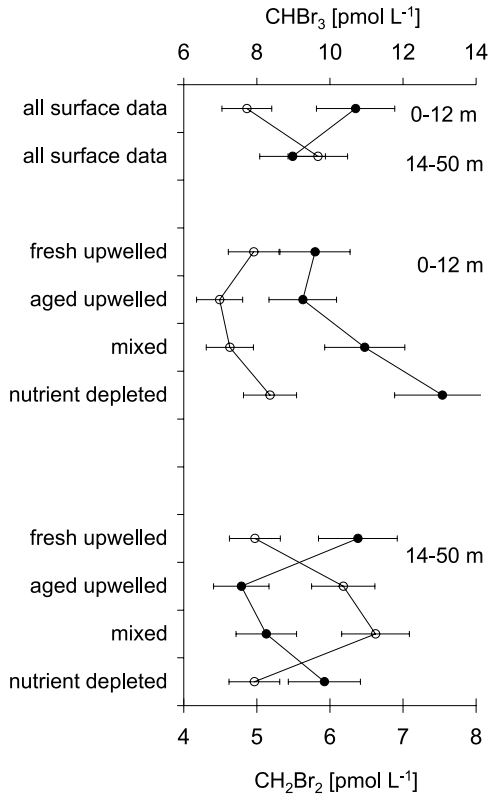

Figure 6. Mean $CHBr_3$ (solid circles) and CH_2Br_2 (open circles) concentrations in different depth ranges (0–12 m and 14–50 m) of the entire data set and of four different SST clusters (see text and Figure 1) from the Mauritanian upwelling.

5.1. Influence of Air-Sea Exchange on the Distribution of $CHBr_3$ and CH_2Br_2 in the Upwelling

[25] The coastal upwelling was identified as a general strong source region of both compounds for the atmosphere, but was also found to be variable and was even an occasional sink for $CHBr_3$ [*Quack et al.*, 2007]. In the region of the lowest sea surface concentrations in the southeast of the Mauritanian upwelling, air to sea fluxes could reach values as high as 3000 pmol m^{-2} hr^{-1} into the ocean [*Quack et al.*, 2007]. The oceanic mixed layer (15–21 m) could during one day of residence time obtain a concentration of 3–5 pmol L^{-1} d^{-1} from the atmosphere, if sea and air distributions represented a steady situation. This high flux could partly explain the concentration increase from fresh upwelled waters to warmer waters (Table 1). However, these extreme air to sea fluxes represent less than 0.1% of the possible air sea fluxes, while the general flux is from the ocean to the atmosphere (mean flux: 1000–2500 pmol m^{-2} hr^{-1}) in the Mauritanian upwelling [*Quack et al.*, 2007]. Thus additional oceanic sources are likely in this region, especially in the warm nutrient-depleted surface waters, where constant oceanic emissions occur. This is also true for CH_2Br_2, where the maximum possible air to sea flux for CH_2Br_2 of 420 pmol m^{-2} hr^{-1} could contribute 0.5 pmol L^{-1} to the mixed layer during one day.

5.2. Physical and Biogeochemical Tracers and the Influence of Advection on the Distribution of $CHBr_3$ and CH_2Br_2 in the Upwelling

[26] $CHBr_3$ concentrations correlated positively with temperature and oxygen while negative correlations were found with nitrate and phosphate in the top 100 m of the upwelling. Coupled with its tendency to increase in higher saline waters (Table 2), this suggests that $CHBr_3$ is introduced to the upwelling waters near the surface.

[27] The rate of photosynthetic oxygen production, calculated from the nitrate decline between the fresh upwelled and the other surface waters by [*Körtzinger et al.*, 2001]

$$O_{2(\text{photosynthetic})}\left[\mu\text{mol L}^{-1}\right] = \left(NO_3^-{}_{\text{cluster}} - NO_3^-{}_{\text{fresh upwelled}}\left[\mu\text{mol L}^{-1}\right]\right)*9.64$$

indicated that oxygen from primary productivity was sufficient to explain the supersaturations of oxygen in all surface water types and that primary production of O_2 dominates over its air-sea exchange.

[28] The coincidence of elevated $CHBr_3$ and the biologically enhanced O_2 concentrations, as well as negative correlations with the biogeochemical tracers nitrate and phosphate thus strongly favor the idea of an active involvement of biological production in the $CHBr_3$ formation. Additionally, $CHBr_3$ concentrations often increase with a relative nitrate loss from the system indicated by [*Gruber and Sarmiento*, 1997]

$$N^* = NO_3^-\left[\mu\text{mol L}^{-1}\right] - 16\ PO_4^{3-}\left[\mu\text{mol L}^{-1}\right] + 2.9$$

likely indicating nitrate uptake during phytoplankton production (Figure 8a). N* as quasi conservative biogeochemical tracer was introduced as indicator for denitrification and nitrogen fixation for deep ocean waters [*Gruber and Sarmiento*, 1997], but shows benefits for the trace gas observations in the surface waters here as well.

[29] In contrast CH_2Br_2 concentrations increase with depth (Tables 1 and 2 and Figure 3) and in waters with an accumulation of excess nitrogen over phosphorus (top 50 m of all water types, Figure 8b), indicating its increase during heterotrophic processes. The different distributions of $CHBr_3$ and CH_2Br_2 and correlations with N* indicate unequal sources and/or fates of the compounds and show that water masses with diverse biogeochemical histories are advected. The role of advection for the compounds in the Mauritanian upwelling is underlined by the dissimilar clustering of the trace gas concentrations and their ratios in different water types, visible in the T/S diagrams (Figure 5).

5.3. Influence of Local Biology on the Distribution of $CHBr_3$ and CH_2Br_2

[30] Among the correlations obtained in our analyses we note especially the lack of correlation of the brominated compounds with the phytoplankton biomass expressed in chlorophyll *a* or fucoxanthin, the marker pigment for diatoms (Table 2). The largest phytoplankton abundance

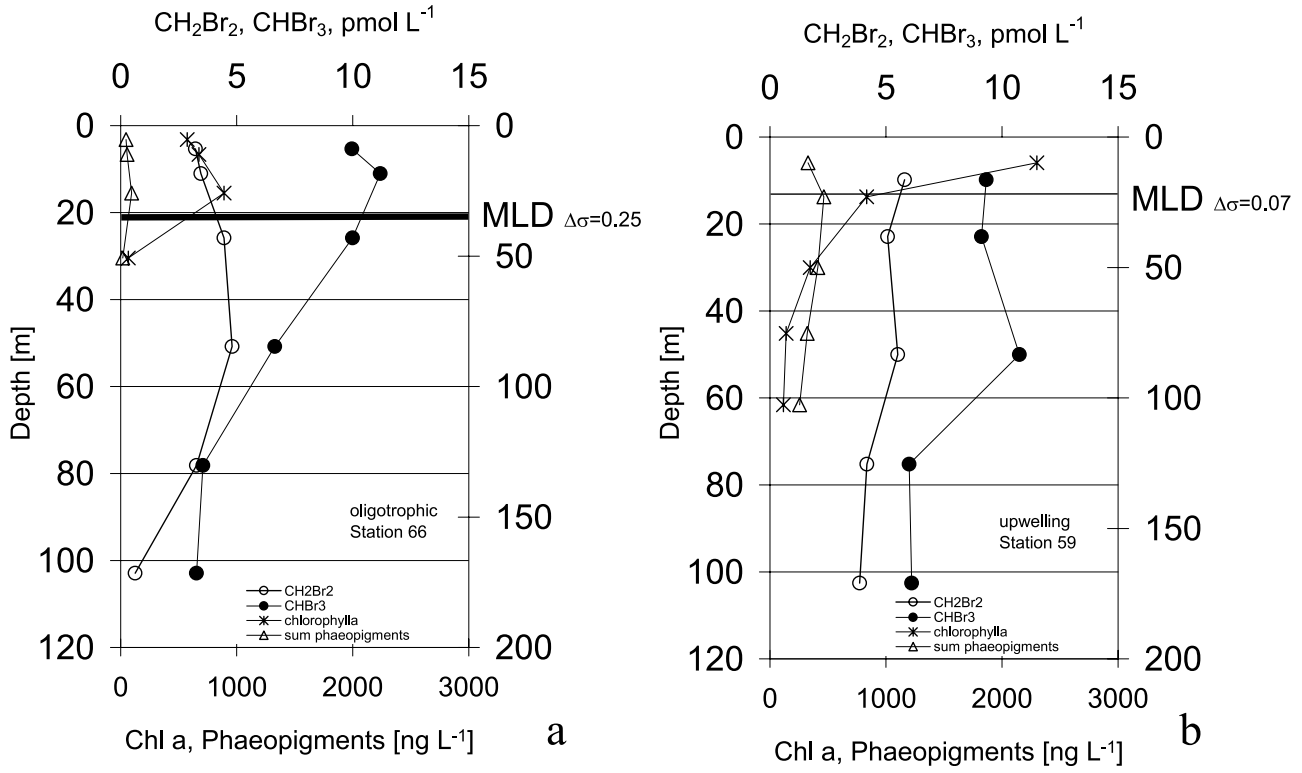

Figure 7. Depth profiles of $CHBr_3$, CH_2Br_2, chl *a*, and phaeopigments (sum of phaeophoride, pyro-phaeophorbide, phaephytin, and pyro-phaeophytin): (a) type A profile at station 66 and (b) type B profile at station 59. Specific mixed layer depth (MLD) (criterion $\Delta\sigma_\theta$ m^{-1}) is also plotted. Bar thickness represents the stratification strength.

in aged upwelled water (cluster 2), which originated mainly from diatoms was not accompanied by elevated $CHBr_3$ or CH_2Br_2 concentrations (Figure 9a).

5.3.1. $CHBr_3$

[31] $CHBr_3$ showed various correlations with phytoplankton pigments in the top 12 and top 100 m of cold and warm waters (Table 2). Although it did not correlate with the high fucoxanthin levels (diatom populations) in aged upwelled waters (Figure 9a), $CHBr_3$ concentrations were correlated with low concentrations of the diatom marker pigment in the mixed water types (Table 2) and also showed positive trends in fresh upwelled and nutrient-depleted warm waters (Figure 9b). The data suggest a weak $CHBr_3$ production in the presence of diatoms, which however are known to produce $CHBr_3$ in the laboratory [*Moore et al.*, 1996]. $CHBr_3$ concentrations were also correlated to phaeopigments, especially the phaeophorbides in different waters (Table 2) indicating that senescence and grazing additionally affect the $CHBr_3$ distribution in the upwelling region.

[32] $CHBr_3$ concentrations were additionally correlated with the cyanobacterial marker pigment zeaxanthin in warm surface waters (Figure 9c and Table 2). This is indicative of miscellaneous biological sources for $CHBr_3$ in the different water types of the Mauritanian upwelling, underlined by its different correlations toward the fucoxanthin to zeaxanthin ratio in cold and warm waters (Figure 9d). That the largest concentrations and supersaturations of $CHBr_3$ occurred in warm nutrient-depleted surface waters (Figure 4 and Table 1), coupled with the correlation of elevated $CHBr_3$ concentrations with zeaxanthin and the coincidence of the largest $CHBr_3$ concentrations with the smallest fucoxanthin to zeaxanthin ratio (Figure 9d) suggests the possible production of $CHBr_3$ by *Synechococcus* in the warm surface waters. Correlations with peridin and chlorophyll *b* in mixed waters indicate that other phytoplankton species may also be involved in the process of $CHBr_3$ production.

[33] The manifold correlations with phytoplankton pigments and the fact that the largest concentrations were found in the warmest surface waters also suggest that the phytoplankton efflux of organic matter could be involved in an abiotic production of $CHBr_3$, which may be kinetically favored in the warmest waters. The abiotic production may occur via the common haloform reaction, where the formation of hypobromite by various oxidants as hydrogen peroxide (in the presence of free peroxidases), hydroxylradicals and ozone under the influence of light is a limiting factor [*Quack and Wallace*, 2003].

5.3.2. CH_2Br_2

[34] A strong correlation of CH_2Br_2 and $CHBr_3$ in nutrient-depleted warm surface waters (Table 2) suggests a common production of both compounds in these waters. Generally however CH_2Br_2 showed different and opposing correlations with pigment concentrations; e.g., peridin and chl *b* and chemical parameters e.g., oxygen and silicate in the various water types (Table 2). This indicates that also other processes are involved in the CH_2Br_2 distribution compared to $CHBr_3$.

[35] In coastal source areas with elevated concentrations of the compounds the $CH_2Br_2/CHBr_3$ ratio frequently is 0.1

Table 2. Matrix of Significant Correlations ($p < 0.5$) of Oceanic $CHBr_3$ and CH_2Br_2 Concentrations and Physical, Chemical, and Biological Variables in Different Depth Ranges (0–12 m and 0–100 m) of Four SST Clusters in the Mauritanian Upwelling[a]

	Lat, °N	Lon, °E	Depth, m	Bottom Depth, m	Temp, °C	Sal	Oxygen, μmol L^{-1}	Nitrate, μmol L^{-1}	Phosphate, μmol L^{-1}	Silicate, μmol L^{-1}	$CHBr_3$, pmol L^{-1}	Sum Chl *a*, ng L^{-1}	Fucoxanthin, ng L^{-1}	Peridin, ng L^{-1}	Zea-xanthin, ng L^{-1}	Chl *b*, ng L^{-1}	Phaeopigments, ng L^{-1}
									$CHBr_3$								
Data of top 12 m of entire stations																	
Cluster 1							0.75			0.78					*−0.74*		
Cluster 2				0.96													0.95
Cluster 3													0.94				0.94
Cluster 4														0.91	0.76		
Data of top 100 m of entire stations	0.26		*−0.46*		0.54		0.39	*−0.47*	*−0.47*						0.33		
Cluster 1		*−0.59*			0.50		0.60			0.63			0.65		*−0.59*		0.73
Cluster 2		*−0.81*															0.73
Cluster 3			*−0.52*		0.46		0.47						0.79			0.72	0.85
Cluster 4		*−0.76*	*−0.56*		0.75		0.53	−0.73	*−0.80*	*−0.78*		0.63			0.82		
									CH_2Br								
Data of top 12 m of entire stations		0.56				*−0.38*											
Cluster 1										*−0.81*	*−0.89*						
Cluster 2																	
Cluster 3	*−0.91*	0.97		*−0.97*		*−0.98*	*−0.97*	0.97	0.99	0.98						*−0.96*	
Cluster 4		0.94		*−0.79*							0.81	0.79		0.86	0.79		0.77
Data of top 100 m of entire stations	*−0.52*	0.33															
Cluster 1										*−0.72*							
Cluster 2																	
Cluster 3	*−0.66*	0.64		*−0.63*		*−0.60*										*−0.76*	
Cluster 4	*−0.53*	0.71		*−0.63*							0.68			*−0.92*			

[a]Cluster 1 (fresh upwelled water, SST 16.7°–18°C), cluster 2 (aged upwelled water, SST 18°C–19°C), cluster 3 (mixed water, SST 19°–21°C), cluster 4 (nutrient-depleted warm water, SST >21°C). Abbreviations are Lat, latitude; Lon, longitude; Temp, temperature; and Sal, salinity. Italic typeface indicates negative correlations.

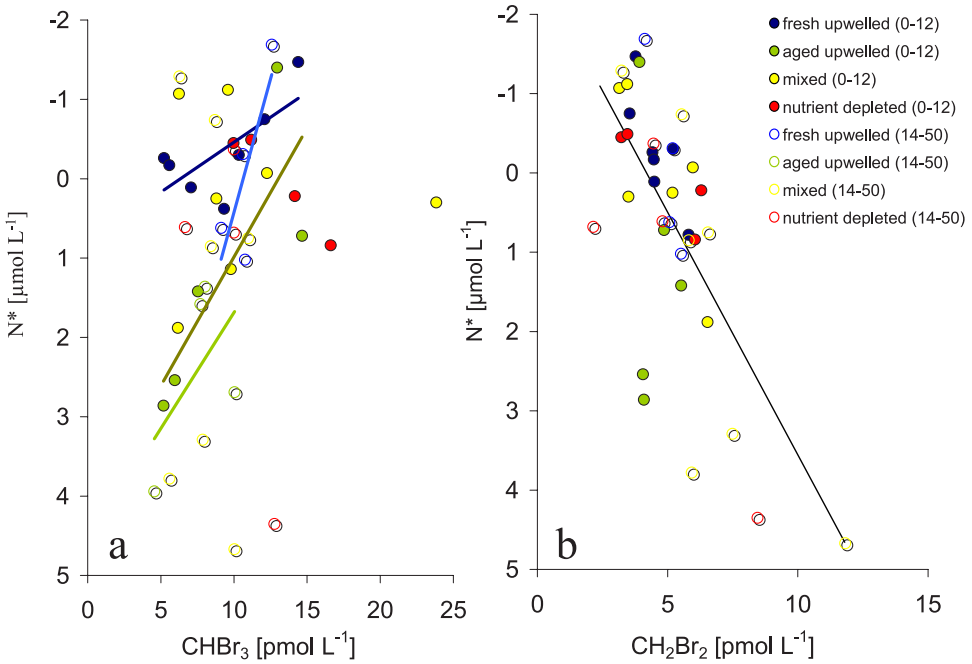

Figure 8. (a) $CHBr_3$ versus N* (N* = $[NO_3^-]$ − 16 $[PO_4^{3-}]$ + 2.9, according to *Gruber and Sarmiento* [1997] and (b) CH_2Br_2 versus N*. Lines indicate characteristic trends (r^2 between 0.62 and 0.67) among the data of fresh (blue) and aged upwelled surface water (green) (Figure 8a) and of the entire data set with an r^2 of 0.55 (Figure 8b). (For color code see Figure 1; solid circles and dark lines indicate data from 0 to 12 m, and open circles and light lines indicate data from 14 to 50 m of the different SST cluster).

or even smaller [e.g., *Carpenter et al.*, 2003; *Moore and Tokarczyk*, 1993; *Krysell and Nightingale*, 1994; *Abrahamsson et al.*, 2004], while in open ocean water the ratio increases to >0.5 [*Butler et al.*, 2007] or even reaches >1 (B. Quack, unpublished data, 2004). This suggests an additional source of CH_2Br_2 compared to $CHBr_3$ in the open ocean and/or a relative stronger sink of $CHBr_3$ compared to CH_2Br_2, being also true for the Mauritanian upwelling where the $CH_2Br_2/CHBr_3$ concentration ratio of 0.4 (0.3–1.1) is also high.

[36] This observation is surprising, first, since $CHBr_3$ is believed to be produced preferentially over CH_2Br_2 and, second, has generally longer lifetimes because of chemical and biological degradation compared to CH_2Br_2 in the oceanic environment [*Vogel et al.*, 1987, *Goodwin et al.*, 1997]. Only the rate of reduction is faster for $CHBr_3$ than for CH_2Br_2. Thus reductive hydrogenolysis, a known loss process of $CHBr_3$, producing CH_2Br_2 from its parent compound under anoxic conditions [*Vogel et al.*, 1987] should be considered as possible source/sink process for the compounds in the upwelling region and the open ocean. A negative correlation with bottom depth, an increase toward coastal waters and positive correlations with nitrate and N* (Table 2) could all be indicators for a production of CH_2Br_2 during a fast heterotrophic process, involving $CHBr_3$ and occurring either in sediments or the water column. This process could explain the relative enhancement of CH_2Br_2 compared to $CHBr_3$ in the Mauritanian shelf region, which is strongly influenced by sediment resuspension and aged water masses which in turn have been influenced by heterotrophic processes. An additional cause for the ratio increase in specifically surface waters could be differential loss of $CHBr_3$ and CH_2Br_2 due to air-sea exchange. While the transfer coefficients of both compounds are similar, a generally greater concentration gradient between air and seawater of $CHBr_3$ compared to that of CH_2Br_2 causes a larger flux of $CHBr_3$ from the ocean to the atmosphere. Over time, this differential loss could increase the $CH_2Br_2/CHBr_3$ ratio as well. At present there is insufficient information to evaluate the relative importance of both processes.

6. Summary and Conclusion

[37] The postulated high concentrations of $CHBr_3$ in the diatom-rich surface waters along the Mauritanian coast [*Quack et al.*, 2004] were not encountered in spring 2005 and the existence of a significant planktonic source for $CHBr_3$ in the Mauritanian upwelling was not supported by the measurements. The highest chlorophyll *a* and diatom concentrations in aged upwelled water were not correlated with high $CHBr_3$ concentrations. However, correlations of $CHBr_3$ with low concentrations of several phytoplankton pigments and oxygen in various water types, as well as negative correlations with nutrients indicate a small $CHBr_3$ production by phytoplankton in the upwelling, with diatoms and cyanobacteria as the likely producers. Correlations of this compound with phaeopigments indicate that death and decay may contribute also. In the warmest surface waters with the highest $CHBr_3$ concentrations abiotic production could be another additional source. In fresh upwelled waters the atmosphere can account for oceanic $CHBr_3$, potentially increasing its concentrations by 20–30%.

[38] Differing correlations of CH_2Br_2 compared to $CHBr_3$ with chemical and biological parameters, opposing distributions toward depth and among the surface waters reveal

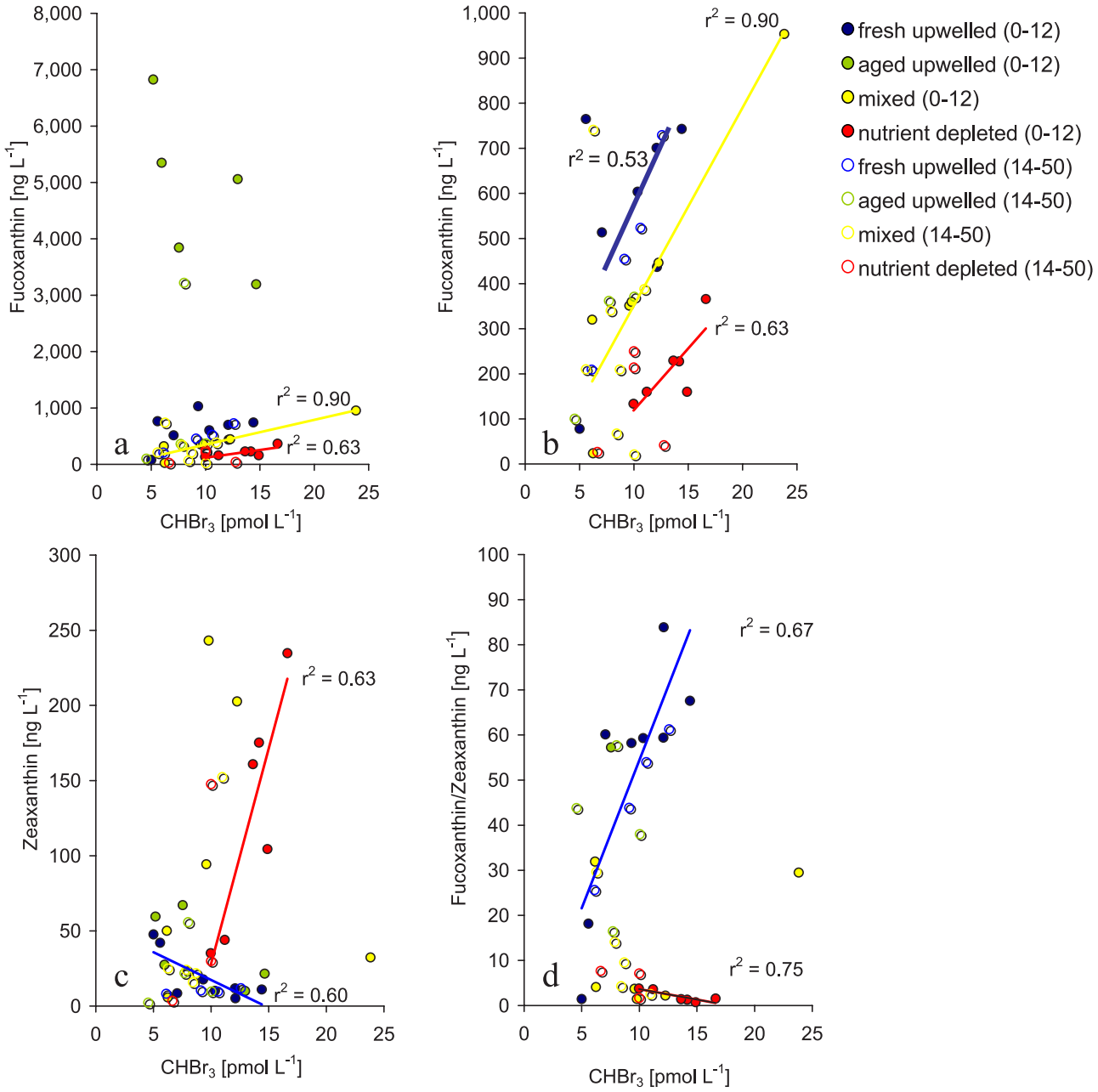

Figure 9. (a) $CHBr_3$ versus fucoxanthin (up to 8000 ng L^{-1}), (b) $CHBr_3$ versus fucoxanthin (up to 1000 ng L^{-1}), (c) zeaxanthin, and (d) fucoxanthin/zeaxanthin ratio in the top 50 m of different SST clusters in the Mauritanian upwelling. Lines indicate characteristic trends among the data of mixed (yellow) water and nutrient-depleted (red) surface water. (For color code see Figure 1; solid circles indicate data from 0 to 12 m, and open circles indicate data from 14 to 50 m).

unequal source and loss processes of both compounds. CH_2Br_2 is enriched over $CHBr_3$ in the upwelling (ratio > 0.4) compared to other coastal source areas with elevated concentrations of both compounds (ratio < 0.1) approaching open ocean ratios (ratio > 0.5). While $CHBr_3$ is closely correlated with production parameters in the surface water, CH_2Br_2 concentrations in contrast increase toward deeper and more heterotrophic water. The observations suggest biologically mediated reductive hydrogenolysis of $CHBr_3$ as a potential source for CH_2Br_2 in the sediments or the water column. A relative importance of this process compared to differential air-sea exchange of the compounds for the increased loss of $CHBr_3$ from surface waters toward the open and the subsurface ocean is likely.

[39] Although the oceanic distributions of $CHBr_3$ and CH_2Br_2 are outlined and correlations and possible sources are discussed, it is not possible to identify the most significant production and distribution mechanism for the compounds in this heterogeneous region. Chlorophyll *a* and diatom marker pigments have to be excluded as reliable proxies for the oceanic distribution of $CHBr_3$ and the link between primary productivity and $CHBr_3$ release is still

unresolved. The relative enrichment of CH_2Br_2 compared to $CHBr_3$ and the possible transformation of $CHBr_3$ to CH_2Br_2 in the open oceanic environment should be further investigated. Lagrangian drift and diurnal process studies should be envisaged for future experiments in the different upwelling regimes (fresh, older, aged) and depth ranges, to further elucidate the oceanic $CHBr_3$ and CH_2Br_2 production and loss processes.

[40] **Acknowledgments.** This work was supported by grants BA 1990/6 and WA 1434/4-1 of the Deutsche Forschungsgemeinschaft (DFG). We acknowledge chief scientist Hermann Bange and the captain and crew of R/V *Poseidon* and wish to thank Annegret Stuhr for microscopy and taxonomy of phytoplankton.

References

Abrahamsson, K., A. Loren, A. Wulff, and S. A. Wängberg (2004), Air-sea exchange of halocarbons: The influence of diurnal and regional variations and distributions of pigments, *Deep Sea Res., Part II*, *51*, 2789–2805.

Atlas, E., W. Pollock, J. Greenberg, L. Heidt, and A. M. Thompson (1993), Alkyl nitrates, nonmethane hydrocarbons, and halocarbon gases over the equatorial Pacific Ocean during Saga 3, *J. Geophys. Res.*, *98*, 16,933–16,947.

Baker, A. R., S. M. Turner, W. J. Broadgate, A. Thompson, G. B. McFiggans, O. Vesperini, P. D. Nightingale, P. S. Liss, and T. D. Jickells (2000), Distribution and sea-air fluxes of biogenic trace gases in the eastern Atlantic Ocean, *Global Biogeochem. Cycles*, *14*, 871–886.

Barlow, R. G., J. Aiken, G. F. Moore, P. M. Holligan, and S. Lavender (2004), Pigment adaptations in surface phytoplankton along the eastern boundary of the Atlantic Ocean, *Mar. Ecol. Prog. Ser.*, *281*, 13–26.

Bartnicki, E. W., and C. E. Castro (1994), Biodehalogenation—Rapid oxidative metabolism of monohalomethanes and polyhalomethanes by *Methylosinus Trichosporium* Ob-3b, *Environ. Toxicol. Chem.*, *13*, 241–245.

Bouwer, E. J., and P. L. McCarty (1983), Transformations of 1-carbon and 2-carbon halogenated aliphatic organic compounds under methanogenic conditions, *Appl. Environ. Microbiol.*, *45*(4), 1286–1294.

Butler, J. H., D. B. King, J. M. Lobert, S. A. Montzka, S. A. Yvon-Lewis, B. D. Hall, N. J. Warwick, D. J. Mondeel, M. Aydin, and J. W. Elkins (2007), Oceanic distributions and emissions of short-lived halocarbons, *Global Biogeochem. Cycles*, *21*, GB1023, doi:10.1029/2006GB002732.

Carpenter, L. J., and P. S. Liss (2000), On temperate sources of bromoform and other reactive organic bromine gases, *J. Geophys. Res.*, *105*, 20,539–20,547.

Carpenter, L. J., P. S. Liss, and S. A. Penkett (2003), Marine organohalogens in the atmosphere over the Atlantic and the Southern oceans, *J. Geophys. Res.*, *108*(D9), 4256, doi:10.1029/2002JD002769.

Class, T. H., and K. Ballschmiter (1988), Chemistry of organic traces in air: Sources and distributions of bromo- and bromochloromethanes in marine air and surface water of the Atlantic Ocean, *J. Atmos. Chem.*, *6*, 35–46.

Demarcq, H., and V. Faure (2000), Coastal upwelling and associated retention indices derived from satellite SST: Application to Octopus vulgaris recruitment, *Oceanol. Acta*, *23*, 391–408.

Fernández, E., E. Marañón, X. A. G. Morán, and P. Serret (2003), Potential causes for the unequal contribution of picoplankton to total biomass and productivity in oligotrophic waters, *Mar. Ecol. Prog. Ser.*, *254*, 101–109.

Geen, C. E. (1992), Selected marine sources and sinks of bromoform and other low molecular weight organobromines, Ph.D. thesis, 109 pp, Dalhousie Univ., Halifax, N. S., Canada.

Gibb, S. W., R. G. Barlow, D. G. Cummings, N. W. Rees, C. C. Trees, P. Holligan, and D. Suggett (2000), Surface phytoplankton pigment distributions in the Atlantic Ocean: An assessment of basin scale variability between 50°N and 50°S, *Prog. Oceanogr.*, *45*, 339–368.

Gibb, S. W., D. G. Cummings, X. Irigoien, R. G. Barlow, and R. F. C. Mantoura (2001), Phytoplankton pigment chemotaxonomy of the northeastern Atlantic, *Deep Sea Res., Part II*, *48*, 795–823.

Goodwin, K. D., M. E. Lidstrom, and R. S. Oremland (1997), Marine bacterial degradation of brominated methanes, *Environ. Sci. Technol.*, *31*, 3188–3192.

Grasshoff, K., K. Kremling, and M. Erhardt (Eds.) (1999), *Methods of Sea Water Analysis*, Wiley-VCH, Weinheim, Germany.

Gruber, N., and J. L. Sarmiento (1997), Global patterns of marine nitrogen fixation and denitrification, *Global Biogeochem. Cycles*, *11*, 235–266.

Hagen, E. (2001), Northwest African upwelling scenario, *Oceanol. Acta*, *24*, 113–128.

Hoffmann, L., I. Peeken, K. Lochte, P. Assmy, and M. Veldhuis (2006), Different reactions of Southern Ocean phytoplankton size classes to iron fertilization, *Limnol. Oceanogr.*, *51*, 1217–1229.

Jeffrey, S. W., R. F. C. Mantoura, and S. W. Wright (1997), *Phytoplankton Pigments in Oceanography: Guidelines to Modern Methods*, *Monogr. Oceanogr. Method*, vol. 10, UNESCO, Paris.

Klick, S., and K. Abrahamsson (1992), Biogenic volatile iodated hydrocarbons in the ocean, *J. Geophys. Res.*, *97*, 12,683–12,687.

Körtzinger, A., J. L. Hedges, and P. D. Quay (2001), Redfield ratios revisited: Removing the biasing effect of anthropogenic CO_2, *Limnol. Oceanogr.*, *46*, 964–970.

Krysell, M., and P. D. Nightingale (1994), Low molecular weight halocarbons in the Humber and Rhine estuaries determined using a new purge-and-trap gas chromatographic method, *Cont. Shelf Res.*, *14*(12), 1311–1329.

Mabey, W., and T. Mill (1978), Critical review of hydrolysis of organic compounds in water under environmental conditions, *J. Phys. Chem. Ref. Data*, *7*, 383–415.

Mackey, M. D., D. J. Mackey, H. W. Higgings, and S. W. Wright (1996), CHEMTAX— A program for estimating class abundances from chemical markers: Application to HPLC measurements of phytoplankton, *Mar. Ecol. Prog. Ser.*, *144*, 265–283.

Manley, S. L., K. Goodwin, and W. J. North (1992), Laboratory production of bromoform, methylene bromide, and methyl-iodide by macroalgae and distribution in nearshore southern California waters, *Limnol. Oceanogr.*, *37*, 1652–1659.

Marañón, E., P. M. Holligan, M. Varela, B. Mouriño, and A. J. Bale (2000), Basin-scale variability of phytoplankton biomass, production and growth in the Atlantic Ocean, *Deep Sea Res., Part I*, *47*, 825–857.

Margaleff, R. (1978), Phytoplankton communities in upwelling areas: The example of NW Africa, *Oecol. Aquat.*, *3*, 97–132.

Minas, H. J., T. T. Packard, M. Minas, and B. Coste (1982), An analysis of the production-regeneration system in the coastal upwelling area off NW Africa based on oxygen, nitrate and ammonium distributions, *J. Mar. Res.*, *40*, 615–641.

Moore, R. M., and R. Tokarczyk (1993), Volatile biogenic halocarbons in the northwest Atlantic, *Global Biogeochem. Cycles*, *7*, 195–210.

Moore, R. M., M. Webb, R. Tokarczyk, and R. Wever (1996), Bromoperoxidase and iodoperoxidase enzymes and production of halogenated methanes in marine diatom cultures, *J. Geophys. Res.*, *101*, 20,899–20,908.

Neidleman, S. L., and J. Geigert (1986), *Biohalogenation: Principles, Basic Roles and Applications*, 200 pp., Ellis Horwood, Chichester, U. K.

Nightingale, P. D., G. Malin, and P. S. Liss (1995), Production of chloroform and other low-molecular-weight halocarbons by some species of macro algae, *Limnol. Oceanogr.*, *40*, 680–689.

Partensky, F., J. Blanchot, F. Lantoine, J. Neveux, and D. Marie (1996), Vertical structure of picoplankton at different trophic sites of the tropical northeastern Atlantic Ocean, *Deep Sea Res., Part I*, *43*, 1191–1213.

Postel, L., and W. Zahn (1987), Einfluß des Nouakchott-Canyons (Mauretanien) auf ozeanologische Feldverteilungen im Marz 1984, 1. Einführung und Meßprogramm, *Beitr. Meeresk.*, *57*, 45–50.

Quack, B., and D. W. R. Wallace (2003), Air-sea flux of bromoform: Controls, rates, and implications, *Global Biogeochem. Cycles*, *17*(1), 1023, doi:10.1029/2002GB001890.

Quack, B., E. Atlas, G. Petrick, V. Stroud, S. Schauffler, and D. W. R. Wallace (2004), Oceanic bromoform sources for the tropical atmosphere, *Geophys. Res. Lett.*, *31*, L23S05, doi:10.1029/2004GL020597.

Quack, B., E. Atlas, G. Petrick, and D. W. R. Wallace (2007), Bromoform and dibromomethane above the Mauritanian upwelling: Atmospheric distributions and oceanic emissions, *J. Geophys. Res.*, *112*, D09312, doi:10.1029/2006JD007614.

Roy, S., and S. A. Poulet (1990), Laboratory study of the chemical composition of aging copepod fecal material, *J. Exp. Mar. Biol. Ecol.*, *135*, 3–18.

Salawitch, R. J., D. K. Weisenstein, L. J. Kovalenko, C. E. Sioris, P. O. Wennberg, K. Chance, M. K. W. Ko, and C. A. McLinden (2005), Sensitivity of ozone to bromine in the lower stratosphere, *Geophys. Res. Lett.*, *32*, L05811, doi:10.1029/2004GL021504.

Salawitch, R. J. (2006), Atmospheric chemistry–Biogenic bromine, *Nature*, *439*, 275–277.

Schauffler, S. M., E. L. Atlas, D. R. Blake, F. Flocke, R. A. Lueb, J. M. Lee-Taylor, V. Stroud, and W. Travnicek (1999), Distributions of brominated organic compounds in the troposphere and lower stratosphere, *J. Geophys. Res.*, *104*, 21,513–21,535.

Tanhua, T., E. Fogelqvist, and O. Basturk (1996), Reduction of volatile halocarbons in anoxic seawater, results from a study in the Black Sea, *Mar. Chem.*, *54*, 159–170.

Theiler, R., J. C. Cook, and L. P. Hager (1978), Halohydrocarbon synthesis by bromoperoxidase, *Science*, *202*, 1094–1096.
Tokarczyk, R., and R. M. Moore (1994), Production of volatile organohalogens by phytoplankton cultures, *Geophys. Res. Lett.*, *21*, 285–288.
Veldhuis, M. J. W., and G. W. Kraay (2004), Phytoplankton in the subtropical Atlantic Ocean: Towards a better understanding of biomass and composition, *Deep Sea Res., Part I*, *51*, 507–530.
Vogel, T. M., C. S. Criddle, and P. L. McCarty (1987), Transformations of halogenated aliphatic compounds, *Environ. Sci. Technol.*, *21*, 722–736.
Wade, L. G., Jr. (1999), *Organic Chemistry*, 4th ed., Prentice-Hall, Upper Saddle River, N. J.
Weikert, H. (1984), Zooplankton distribution and hydrography in the Mauritanian upwelling region off northwestern Africa, with special reference to the calanoid copepods, *Meeresforschung*, *30*, 155–171.
World Meteorological Organization (2007), Scientific assessment of ozone depletion: 2006, *Global Ozone Res. Monit. Proj. 50*, 498 pp., Geneva, Switzerland.
Yang, X., R. A. Cox, N. J. Warwick, J. A. Pyle, G. D. Carver, and N. H. Savage (2005), Tropospheric bromine chemistry and its impacts on ozone: A model study, *J. Geophys. Res.*, *110*, D23311, doi:10.1029/2005JD006244.

K. Nachtigall, I. Peeken, G. Petrick, and B. Quack, Department of Marine Biogeochemistry, Leibniz Institute of Marine Sciences, Kiel, Düsternbrooker Weg 20, Kiel D-24105, Germany. (bquack@ifm-geomar.de)